DNA Hydrogels

International Edition: DOI: 10.1002/anie.201610125
German Edition: DOI: 10.1002/ange.201610125

Clamped Hybridization Chain Reactions for the Self-Assembly of Patterned DNA Hydrogels

Jianbang Wang[+], Jie Chao[+], Huajie Liu, Shao Su, Lianhui Wang, Wei Huang, Itamar Willner, and Chunhai Fan*

Abstract: *DNA hydrogels hold great potential for biological and biomedical applications owing to their programmable nature and macroscopic sizes. However, most previous studies involve spontaneous and homogenous gelation procedures in solution, which often lack precise control. A clamped hybridization chain reaction (C-HCR)-based strategy has been developed to guide DNA self-assembly to form macroscopic hydrogels. Analogous to catalysts in chemical synthesis or seeds in crystal growth, we introduced DNA initiators to induce the gelation process, including crosslinked self-assembly and clamped hybridization in three dimensions with spatial and temporal control. The formed hydrogels show superior mechanical properties. The use of printed, surface-confined DNA initiators was also demonstrated for fabricating 2D hydrogel patterns without relying on external confinements. This simple method can be used to construct DNA hydrogels with defined geometry, composition, and order for various bioapplications.*

Molecular self-assembly is a universal phenomenon in nature,[1] which happens in systems ranging from inorganic to organic, and has inspired researchers to create artificial complex and functional materials.[2] Among various molecules, DNA is an excellent candidate for intelligent constructions owing to its prominent sequence programmability and self-recognition ability.[3] To date, numerous static and dynamic DNA self-assembled nanostructures have been created.[4] Beyond nanoscale, the precise DNA-based self-assembly has also been exploited for constructing macroscopic hydrogels,[5] where the unconstrained crosslinking of DNA building blocks leads to three-dimensional (3D) expanding of hybridizations to random networks. Typically, DNA hydrogels have unique features, such as designable responsiveness,[5h,6] biodegradability,[5f,j,6e,7] encapsulation[5b,8] and selective permeability,[5f] thus have been found promising for both biological and materials sciences. However, most reported methods for making DNA hydrogels are based on simple spontaneous and homogenous gelation processes, namely, the self-assembly of building blocks occurs non-specifically in the whole solution and the efficiency of sol–gel transition is equal everywhere. The selectivity and order of the self-assembly in these one-pot reactions often lack precise control.

Recently, inspired from several well-developed strategies used in chemical synthesis, the concepts of catalyst-assist and field-assist have been introduced to promote the research on synthetic molecular self-assembly.[9] When self-assembly is selectively triggered and regulated by certain stimuli, the controllability and order can be enhanced, which are important for programmable and intelligent assembly. Typically, linear or dendritic DNA hybridization chain reaction (HCR) was employed to construct nanostructures with the help of DNA initiators.[10] This strategy was recently applied, together with acrylamide polymerization and acrylamide–acrydite DNA crosslinking, to construct hybrid DNA–polymer hydrogels that are responsive to certain ions and show switchable electrocatalytic properties.[11] Herein, we developed a new approach for constructing all-DNA hydrogels by a clamped hybridization chain reaction (C-HCR). The sol–gel transition in this design is selectively triggered by a small piece of DNA initiator. However, the clamped core in this C-HCR system, working in a way similar to seeds for crystal growth, enables the bridging and locking the DNA branches. Accordingly, downstream hybridization and crosslinking occur and result in expanded and clamped 3D networks. Importantly, this method enables spatial and temporal control in the gelation process. We demonstrated that 2D DNA hydrogel patterns with defined shapes were achieved on printed DNA initiators arrays without relying on external confinements.

As illustrated in Figure 1, our DNA hydrogel was formed through a clamped hybridization chain reaction, which is different from reported linear and non-linear HCR systems.[10] Like traditional HCR, three DNA strands were used in this system: hairpin strands **H1**, **H2** and initiator strand **I** (Figure 1a). **H1** is a unique component for C-HCR system since it has ten palindromic bases at the 5′ end (segment d). After annealing, two **H1** strands could form a hairpin-dimer through the hybridization of their palindromic segments. **H1**-dimer and **H2** coexist metastably in the absence of initiator **I**

[*] J. Wang,[+] Prof. Dr. H. Liu, Prof. Dr. C. Fan
Division of Physical Biology & Bioimaging Center, Shanghai Synchrotron Radiation Facility, CAS Key Laboratory of Interfacial Physics and Technology, Shanghai Institute of Applied Physics, Chinese Academy of Sciences
Shanghai 201800 (China)
E-mail: liuhuajie@sinap.ac.cn
Prof. Dr. J. Chao,[+] Dr. S. Su, Prof. Dr. L. Wang, Prof. Dr. W. Huang
Key Laboratory for Organic Electronics & Information Displays (KLOEID), Institute of Advanced Materials (IAM) and School of Materials Science and Engineering, Nanjing University of Posts & Telecommunications Institution
9 Wenyuan Road, Nanjing 210046 (China)
Prof. Dr. I. Willner
Institute of Chemistry, The Hebrew University of Jerusalem
Jerusalem 91904 (Israel)
[+] These authors contributed equally to this work.
Supporting information for this article can be found under: http://dx.doi.org/10.1002/anie.201610125.

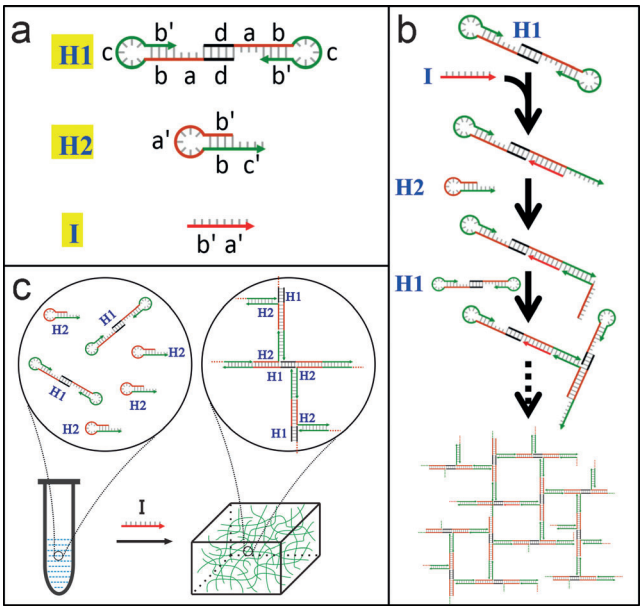

Figure 1. Design principle of the DNA initiator triggered self-assembly process. a) Structures of the hairpin strands **H1**-dimer and **H2**, and initiator strand **I**. b) Details of the C-HCR process initiated by **I**. c) Representation of the gelation process.

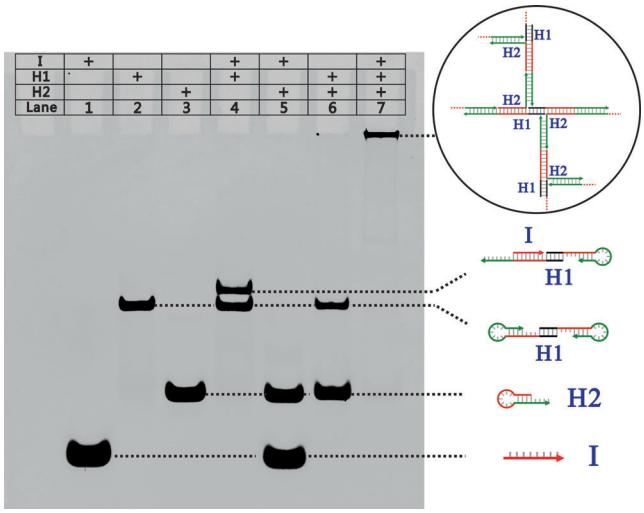

Figure 2. Polyacrylamide gel electrophoresis (PAGE) analysis of the self-assembly behaviors. Lanes 1–3 are **I**, **H1**-dimer, and **H2**, respectively. Lanes 4–7 are different combinations of **I**, **H1**-dimer, and **H2**. All samples were incubated at room temperature overnight and then analyzed with 10% native PAGE.

since long stems (b-b′: 18 bases in **H1** and **H2**) protected short loops (c: 6 bases in **H1** and a′: 10 bases in **H2**) to avoid their hybridizations with toeholds (a in **H1** and c′ in **H2**). Figure 1b shows the details of this C-HCR process. Once a small amount of initiator **I** is added to the mixture of **H1**-dimer and **H2** (**H1**/**H2**:**I** = 50:1), **I** first binds to the toehold region of **H1** and opens the long stem and short loop through DNA strand displacement reaction. Next the active **H1** opens and activates a **H2** through the same mechanism and then the latter will open another **H1** in turn. Importantly, since one **H1**-dimer has two branches, it can form a three-arm junction (with one **I** and one **H2**) or a four-arm junction (with two **H2**) for downstream divergent chain reactions. The hybridizations between **H1**-dimer and **H2** can finally lead to clamped 3D networks, namely DNA hydrogels (Figure 1c). Initiator **I** is working as the stimulus for the sol–gel transition and **I**-**H1**-dimer complex is the nucleus for the network growth.

To verify the design, native polyacrylamide gel electrophoresis (PAGE) was used to analyze the hybridization behaviors of these DNA strands. As shown in Figure 2, lanes 1–3 are **I**, **H1** and **H2** samples, respectively, while lanes 4–7 are varied combinations of them. We note that **H1** and **H2** have nearly the same length but the former in lane 2 migrated much slower than the latter in lane 3, confirming the formation of **H1**-dimer with high efficiency. The incubation of excess **H1**-dimer with a small amount of initiator **I** could form a new band with lower mobility appeared in lane 4. The new band is believed to be the 1:1 complex of **I**-**H1**-dimer, which is highly active for downstream hybridization with **H2**. As control experiments, no hybridizations were found between **I** and **H2** (lane 5), and **H1** and **H2** (lane 6). The incubation of all these three components together resulted in the formation of high-molecular-weight polymers that cannot move freely in the gel (lane 7). Similar phenomenon was observed in agarose gel electrophoresis analysis, except the appearance of a smearing band (Supporting Information, Figure S1). These results are in good accordance with the design that clamped hybridization reactions occur upon the addition of initiator **I** to the mixture of **H1**-dimer and **H2**.

Next we carried out the test in an amplified system to examine whether the activation and hybridization can lead to the formation of macroscopic DNA hydrogels. A solution of **H1**-dimer (600 μM **H1** strands equal 300 μM dimers) and **H2** (600 μM) were prepared in 1X TAE-Mg^{2+} buffer with a volume of 90 μL (2.0 wt% DNA). After a 2-day incubation at room temperature, this pre-gelation solution was still stable and fluidic. A small amount of **I** was then utilized to trigger the sol–gel transition. After an overnight incubation, the sample lost its fluidity and appeared to be gel-like in a 1.5 mL tube (Figure 3a; Supporting Information, Figure S2a). Its gel-like behavior could be observed more clearly after taking it out of the tube with a pipette tip, where an irregular piece of this transparent DNA hydrogel stuck to the tip (Figure 3c). Like other reported DNA hydrogels,[5b,12] our hydrogel has also the ability of trapping gold nanoparticles in its networks, while it showed a color of transparent red (Figure 3b; Supporting Information, Figure S2b). The structural features of this hydrogel were characterized by scanning electron microscopy (SEM) and atomic force microscopy (AFM) at different scales, respectively. From the SEM characterization, the dehydrated sample showed a typical 3D crosslinked morphology (Figure 3d). To reveal details, the average pore size of this hydrogel was further measured to be of about 40.9 nm by using AFM according to a previously reported method.[13] Hydrogels with higher DNA concentrations were also characterized in the same way. Comparing with the values calculated from a rough model,[14] the measured sizes are about three times larger, nevertheless show the same

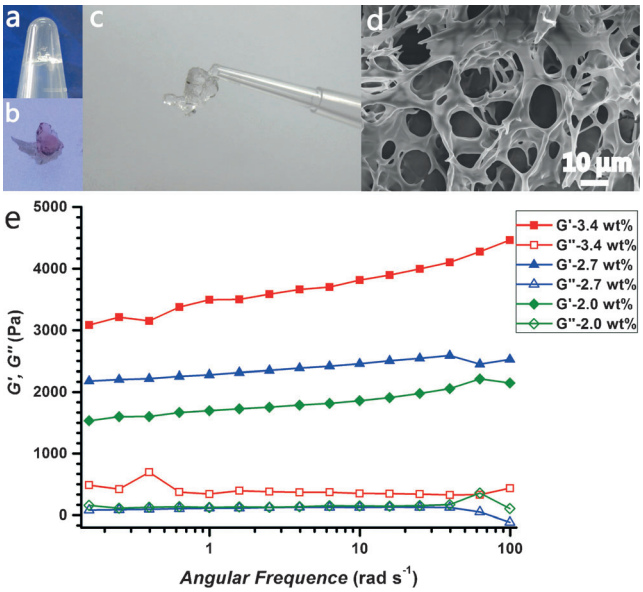

Figure 3. Morphological characterizations and rheology tests of the DNA hydrogels. a) DNA hydrogel formed in a 1.5 mL tube. b) AuNPs (10 nm in diameter) trapped in DNA hydrogel, showing the typical red color. c) A photograph showing a piece of DNA hydrogel stuck to a pipette tip. d) An SEM image showing the inner structure of a dehydrated DNA hydrogel. The hydrogels shown in (a)–(d) have a concentration of 2.0 wt% DNA. e) Frequency sweep tests were carried out between 0.05 and 100 rad s^{-1} at a fixed strain of 1% at 25 °C.

proportional relationship (Supporting Information, Figure S3).

The mechanical property of a hydrogel is important for its functions and applications. Rheology tests were then applied to quantitatively characterize the mechanical strength. From Figure 3e, for the sample with 2.0 wt% DNA (600 μM **H1** and **H2**), its shear-storage modulus (G′) was significantly higher than the shear-loss modulus (G″) in a frequency sweep test, confirming its nature of a true gel. To investigate whether its strength could change with time, an oscillatory time sweep test was conducted and the results showed that this hydrogel was stable and no structural rearrangements occurred (Supporting Information, Figure S4). Furthermore, depending on the DNA amount in the sample, the strength of the formed hydrogel also varied. The G′ was below 2000 Pa in the entire frequency sweep range for 2.0 wt% DNA but gradually increased to above 2000 Pa (2.7 wt% DNA, 800 μM **H1** and **H2**) and 3000 Pa (3.4 wt% DNA, 1000 μM **H1** and **H2**) when more DNA was used (Figure 3e). Notably, compared with reported all-DNA hydrogels containing similar amount of DNA,[12,13,15] our samples possess better mechanical strength. The DNA amount-dependent G′ and G″ values measured at a fixed frequency (1 Hz) and strain (1%) are summarized and compared in the Supporting Information, Figure S5. All G′ values are higher than their corresponding G″ values. The data also reveal that hydrogel could form with as low as 0.7 wt% DNA. On the contrary, the control sample without initiator **I** shows a typical fluidic property even with a high DNA amount of 3.4 wt%.

Using a hydrogel sample with 2.0 wt% DNA, the minimum time required for gelation was also determined with rheology tests. From the Supporting Information, Figure S6, it was found that only 2 h was sufficient for the hydrogel formation since the G′ became significantly higher than the G″.

This initiator-triggered self-assembly strategy has one special feature that the hybridization reactions are started precisely around initiator strands. Like seeds used for crystal growth, **I**-**H1**-dimer complexes are then working as nuclei for the downstream growth of 3D DNA networks. This feature offers possibilities for controlling gelation positions and constructing DNA hydrogel patterns with predefined shapes. As shown in Figure 4a, a design towards exploring the feasibility of substrate-supported hydrogel pattern formation was conceived. Based on the consideration that the hydrogel growth is started and expanded from the initiator strands immobilized on substrate, the final formed hydrogel will keep its shape with the pattern of the immobilized initiators. Notably, no external confinement is needed for the hydrogel pattern growth.

In this design, two HCR processes have been employed. A pre-gelation linear HCR process is first used to enrich the initiators on the printed area and afterwards a C-HCR process will be carried out for the formation of hydrogel patterns. In the first step of this design, streptavidin molecules are spotted on an aldehyde groups coated glass slide into predefined shapes. In the next immobilization step, biotin-modified strands $\mathbf{I_h}$ working as initiators for the linear HCR will be added to bind to streptavidin on the slide. Two hairpin strands (**h1** and **h2-I**) are then used to drive the linear HCR

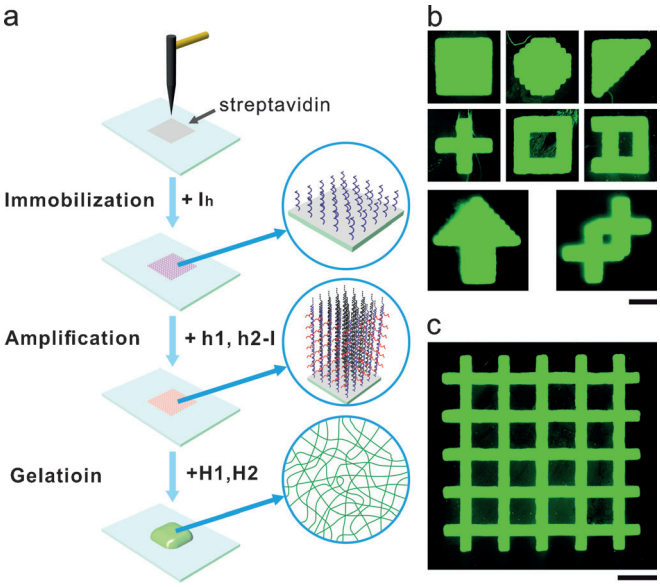

Figure 4. Surface-initiated DNA hydrogel formation. a) Illustration of the gelation process on a glass slide. b) Fluorescence images of polygon patterns of hydrogels, including five simple polygons (without holes, three convex polygons: square, quasi-circle, triangle, and two concave polygons: cross and arrow) and three complex polygons (with holes, two square-based hollow polygons and a DNA duplex-mimic). Scale bar: 500 μm. c) Fluorescence image of a big grid pattern. Scale bar: 1 mm.

(Supporting Information, Figure S7a,b). Each **h2-I** strand contains one I domain, which is the initiator for the C-HCR. After this amplification step, a mixture of **H1** and **H2** is finally incubated with the immobilized C-HCR initiators on the slide. To help visualize the result, a random Cy3-labeled strand that cannot interact with all strands used in the linear HCR and C-HCR systems will be incorporated in this mixture.

To examine the design, the pre-gelation linear HCR process was first optimized to enable loading a large amount of initiators on the substrate (Supporting Information, Figure S7c–e). We found that 2 pmol initiator $\mathbf{I_h}$ for a 1 mm^2 pattern was enough and the **h1/h2-I** to $\mathbf{I_h}$ ratio was chosen as 3.46×10^3:1. Similar to the gelation in tube, the overnight C-HCR process was then carried out with a solution of **H1** and **H2** of 600 μM (**H1**/**H2**:**h2-I** = 1.03×10^4:1), which is efficient for the gelation on the substrate (Supporting Information, Figure S8). To show the robustness and generality of this strategy, eight different polygon patterns with sizes of 1×1 or 1.5×1.5 mm^2 including both simple polygons (without holes) and complex polygons (with holes) were tested. From the images shown in Figure 4b, after incubation and repeated rinsing with buffer to eliminate unspecific bindings on the substrate, fluorescent patterns appeared and no strong fluorescent signals were found on other areas. Their contours are recognizable and match the expectations. As a control experiment, three chosen simple polygons were also prepared with only the C-HCR process but omitting the pre-gelation linear HCR (Supporting Information, Figure S9). Obviously, the gelation degree in these patterns is low, confirming the necessity of the enrichment of initiators in the pre-gelation HCR. Using the same method, a large grid pattern with a size of 5×5 mm^2 was also constructed successfully (Figure 4c). Employing confocal microscopy, the thickness of the substrate-supported hydrogel was measured. As shown in the Supporting Information, Figure S10, a typical thickness of 9.5 μm at the cross-section was observed from both bright field and fluorescence images. We further tested its stability in solution and found that only slight deformation occurred at corners for a square pattern after immersion in 1X TAE-Mg^{2+} buffer for up to 4 h (Supporting Information, Figure S11). This result is in coincidence with the data obtained from Young's modulus characterizations, which revealed that the stiffness in the center is moderately higher than that at the corner (Supporting Information, Figure S12), implying the small difference in the degree of gelation.

In summary, we developed a new strategy of using small amount of DNA initiators to trigger the formation of macroscopic hydrogel. We have demonstrated that, with simple modifications, C-HCR-based DNA hybridization can induce the self-assembly of 3D networks with high efficiency and controllability. Notably, as a proof-of-concept study, 2D DNA hydrogel patterns without external confinements have been achieved for the first time. Given that the DNA initiators employed in this strategy can be flexibly designed, its combination with functional nucleic acids should enable many applications in diagnosis and therapy. Furthermore, DNA modified with special peptide can be used as extracellular matrix for cellular culture.[16] We envisage that surface-confined, patterned, DNA hydrogels could provide, in the future, functional matrices for the spatially controlled growth of cells, and provide chip-based structures for the assembly of cellular networks.[17]

Experimental Section

DNA sequences **H1** (5′-GAT CGC GAT CCT GGC TCC TGT GAT TGT GCT CTA GAC ATC GCT AGA GCA CAA TCA CAG G-3′), **H2** (5′-CTA GAG CAC AAT CAC AGG AGC CAG TTT TCC TGT GAT TGT GCT CTA GCG ATG T-3′, **I** (5′-CTA GAG CAC AAT CAC AGG AGC CAG-3′), and others (see the Supporting Information, Table S1) were used in this study. When making hydrogels, the concentrations for **H1** and **H2** were 50-fold higher than that of initiator **I** and they were dissolved in 1X TAE-Mg^{2+} buffer (40 mM Tris, 20 mM acetic acid, 2 mM EDTA, 12.5 mM Mg^{2+}, pH 8.0) with a volume of 90 μL. The mixture was kept at room temperature overnight for gelation. The rheology tests were preformed using an AR2000ex rheometer (TA Instruments). For constructing DNA hydrogel patterns on glass slide, streptavidin molecules were first spotted onto an aldehyde glass slide using a SpotBot 2 microarrayer programmed by SpotApp software. The arrayed slide was treated with an incubation-blocking-washing process. The slide was then incubated with $\mathbf{I_h}$ strands, which is the initiator for the linear HCR process. Afterwards a solution of **h1** and **h2-I** was used for the amplification of initiators for the next C-HCR process. Finally the slide was incubated with a pre-gelling solution (600 μM **H1**, 600 μM **H2**, 2 μM **F**) and kept at room temperature for gelation. After incubation at room temperature overnight, the slide was gently washed for three times using 1X TAE-Mg^{2+} buffer and dried in air. Hydrogel patterns were imaged using a chip scanner (Genepix 4100A Microarray Fluorescent Scanner).

Acknowledgements

The work was financially supported by the National Basic Research Program of China (973 Program, 2013CB932803, 2013CB933802), the National Natural Science Foundation of China (21473236, 21375139, 21227804, 31371015), and the Chinese Academy of Sciences.

Conflict of interest

The authors declare no conflict of interest.

Keywords: DNA hydrogels · DNA nanotechnology · nucleic acid hybridization · self-assembly · sol–gel process

[1] G. M. Whitesides, B. Grzybowski, *Science* **2002**, *295*, 2418 – 2421.
[2] a) E. Katz, I. Willner, *Angew. Chem. Int. Ed.* **2004**, *43*, 6042 – 6108; *Angew. Chem.* **2004**, *116*, 6166 – 6235; b) H. B. Jin, W. Huang, X. Y. Zhu, Y. F. Zhou, D. Y. Yan, *Chem. Soc. Rev.* **2012**, *41*, 5986 – 5997; c) G. Lu, Y. Li, H. Guo, W. Du, X. Huang, *Polym. Chem.* **2013**, *4*, 3132 – 3139; d) A. Demortiere, A. Snezhko, M. V. Sapozhnikov, N. Becker, T. Proslier, I. S. Aranson, *Nat. Commun.* **2014**, *5*, 3117; e) G. Zan, Q. Wu, *Adv. Mater.* **2016**, *28*, 2099 – 2147.
[3] a) N. C. Seeman, *Nature* **2003**, *421*, 427 – 431; b) M. R. Jones, N. C. Seeman, C. A. Mirkin, *Science* **2015**, *347*, 1260901.

[4] a) Y. Krishnan, F. C. Simmel, *Angew. Chem. Int. Ed.* **2011**, *50*, 3124 – 3156; *Angew. Chem.* **2011**, *123*, 3180 – 3215; b) S. F. J. Wickham, J. Bath, Y. Katsuda, M. Endo, K. Hidaka, H. Sugiyama, A. J. Turberfield, *Nat. Nanotechnol.* **2012**, *7*, 169 – 173; c) Y. Fu, J. Chao, H. Liu, C. Fan, *Chin. Sci. Bull.* **2013**, *58*, 2646 – 2650; d) F. Zhang, J. Nangreave, Y. Liu, H. Yan, *J. Am. Chem. Soc.* **2014**, *136*, 11198 – 11211; e) B. Liu, X. Ouyang, J. Chao, H. Liu, Y. Zhao, C. Fan, *Chin. J. Chem.* **2014**, *32*, 137 – 141; f) Y. Ke, L. L. Ong, W. Sun, J. Song, M. Dong, W. M. Shih, P. Yin, *Nat. Chem.* **2014**, *6*, 994 – 1002; g) A. Kuzuya, Y. Ohya, *Acc. Chem. Res.* **2014**, *47*, 1742 – 1749; h) A. A. Hariri, G. D. Hamblin, Y. Gidi, H. F. Sleiman, G. Cosa, *Nat. Chem.* **2015**, *7*, 295 – 300; i) Z. Liu, C. Tian, J. Yu, Y. Li, W. Jiang, C. Mao, *J. Am. Chem. Soc.* **2015**, *137*, 1730 – 1733.

[5] a) S. H. Um, J. B. Lee, N. Park, S. Y. Kwon, C. C. Umbach, D. Luo, *Nat. Mater.* **2006**, *5*, 797 – 801; b) T. Liedl, H. Dietz, B. Yurke, F. C. Simmel, *Small* **2007**, *3*, 1688 – 1693; c) N. Park, S. H. Um, H. Funabashi, J. Xu, D. Luo, *Nat. Mater.* **2009**, *8*, 432 – 437; d) J. B. Lee, S. Peng, D. Yang, Y. H. Roh, H. Funabashi, N. Park, E. J. Rice, L. Chen, R. Long, M. Wu, D. Luo, *Nat. Nanotechnol.* **2012**, *7*, 816 – 820; e) J. Hur, K. Im, S. Hwang, B. Choi, S. Kim, S. Hwang, N. Park, K. Kim, *Sci. Rep.* **2013**, *3*, 1282; f) J. Jin, Y. Xing, Y. Xi, X. Liu, T. Zhou, X. Ma, Z. Yang, S. Wang, D. Liu, *Adv. Mater.* **2013**, *25*, 4714 – 4717; g) Z. Zhang, S. Li, N. Chen, C. Yang, Y. Wang, *Biomacromolecules* **2013**, *14*, 1174 – 1180; h) L. Zhang, J. Lei, L. Liu, C. Li, H. Ju, *Anal. Chem.* **2013**, *85*, 11077 – 11082; i) A. Zinchenko, Y. Miwa, L. I. Lopatina, V. G. Sergeyev, S. Murata, *ACS Appl. Mater. Interfaces* **2014**, *6*, 3226 – 3232; j) M. Nishikawa, K. Ogawa, Y. Umeki, K. Mohri, Y. Kawasaki, H. Watanabe, N. Takahashi, E. Kusuki, R. Takahashi, Y. Takahashi, Y. Takakura, *J. Controlled Release* **2014**, *180*, 25 – 32; k) X. Wei, T. Tian, S. Jia, Z. Zhu, Y. Ma, J. Sun, Z. Lin, C. J. Yang, *Anal. Chem.* **2015**, *87*, 4275 – 4282; l) H. Qi, M. Ghodousi, Y. Du, C. Grun, H. Bae, P. Yin, A. Khademhosseini, *Nat. Commun.* **2013**, *4*, 2275; m) J. Ren, Y. Hu, C.-H. Lu, W. Guo, M. Aleman-Garcia, F. Ricci, I. Willner, *Chem. Sci.* **2015**, *6*, 4190 – 4195; n) Y. Hu, W. Guo, J. Kahn, M. Aleman-Garcia, I. Willner, *Angew. Chem. Int. Ed.* **2016**, *55*, 4210 – 4214; *Angew. Chem.* **2016**, *128*, 4282 – 4286.

[6] a) H. Yang, H. Liu, H. Kang, W. Tan, *J. Am. Chem. Soc.* **2008**, *130*, 6320 – 6321; b) Y. Zhao, X. Zhao, B. Tang, W. Xu, J. Li, L. Hu, Z. Gu, *Adv. Funct. Mater.* **2010**, *20*, 976 – 982; c) R. Liu, Y. Huang, Y. Ma, S. Jia, M. Gao, J. Li, H. Zhang, D. Xu, M. Wu, Y. Chen, Z. Zhu, C. Yang, *ACS Appl. Mater. Interfaces* **2015**, *7*, 6982 – 6990; d) J. Song, K. Im, S. Hwang, J. Hur, J. Nam, G. O. Ahn, S. Hwang, S. Kim, N. Park, *Nanoscale* **2015**, *7*, 9433 – 9437; e) S. Lilienthal, Z. Shpilt, F. Wang, R. Orbach, I. Willner, *ACS Appl. Mater. Interfaces* **2015**, *7*, 8923 – 8931; f) J. Li, C. Zheng, S. Cansiz, C. Wu, J. Xu, C. Cui, Y. Liu, W. Hou, Y. Wang, L. Zhang, I.-t. Teng, H.-H. Yang, W. Tan, *J. Am. Chem. Soc.* **2015**, *137*, 1412 – 1415; g) W. Guo, C.-H. Lu, R. Orbach, F. Wang, X.-J. Qi, A. Cecconello, D. Seliktar, I. Willner, *Adv. Mater.* **2015**, *27*, 73 – 78.

[7] a) J. Conde, N. Oliva, N. Artzi, *Proc. Natl. Acad. Sci. USA* **2015**, *112*, E1278 – E1287; b) M. Shin, J. H. Ryu, J. P. Park, K. Kim, J. W. Yang, H. Lee, *Adv. Funct. Mater.* **2015**, *25*, 1270 – 1278.

[8] a) H. Kang, H. Liu, X. Zhang, J. Yan, Z. Zhu, L. Peng, H. Yang, Y. Kim, W. Tan, *Langmuir* **2011**, *27*, 399 – 408; b) R. Hu, H. Yuan, B. Wang, L. Liu, F. Lv, S. Wang, *ACS Appl. Mater. Interfaces* **2014**, *6*, 11823 – 11828.

[9] Y. Wang, H.-X. Lin, L. Chen, S.-Y. Ding, Z.-C. Lei, D.-Y. Liu, X.-Y. Cao, H.-J. Liang, Y.-B. Jiang, Z.-Q. Tian, *Chem. Soc. Rev.* **2014**, *43*, 399 – 411.

[10] a) R. M. Dirks, N. A. Pierce, *Proc. Natl. Acad. Sci. USA* **2004**, *101*, 15275 – 15278; b) P. Yin, H. M. T. Choi, C. R. Calvert, N. A. Pierce, *Nature* **2008**, *451*, 318 – 322; c) H. Chandran, A. Rangnekar, G. Shetty, E. A. Schultes, J. H. Reif, T. H. LaBean, *Biotechnol. J.* **2013**, *8*, 221 – 227; d) F. Xuan, I. M. Hsing, *J. Am. Chem. Soc.* **2014**, *136*, 9810 – 9813; e) J. Sadowski, C. Calvert, D. Zhang, N. Pierce, P. Yin, *ACS Nano* **2014**, *8*, 3251 – 3259; f) Z. Nie, P. Wang, C. Tian, C. Mao, *Angew. Chem. Int. Ed.* **2014**, *53*, 8402 – 8405; *Angew. Chem.* **2014**, *126*, 8542 – 8545.

[11] J. Kahn, A. Trifonov, A. Cecconello, W. Guo, C. Fan, I. Willner, *Nano Lett.* **2015**, *15*, 7773 – 7778.

[12] E. Cheng, Y. Xing, P. Chen, Y. Yang, Y. Sun, D. Zhou, L. Xu, Q. Fan, D. Liu, *Angew. Chem. Int. Ed.* **2009**, *48*, 7660 – 7663; *Angew. Chem.* **2009**, *121*, 7796 – 7799.

[13] T. Nöll, H. Schönherr, D. Wesner, M. Schopferer, T. Paululat, G. Nöll, *Angew. Chem. Int. Ed.* **2014**, *53*, 8328 – 8332; *Angew. Chem.* **2014**, *126*, 8468 – 8472.

[14] S. A. Fisher, P. N. Anandakumaran, S. C. Owen, M. S. Shoichet, *Adv. Funct. Mater.* **2015**, *25*, 7163 – 7172.

[15] Y. Xing, E. Cheng, Y. Yang, P. Chen, T. Zhang, Y. Sun, Z. Yang, D. Liu, *Adv. Mater.* **2011**, *23*, 1117 – 1121.

[16] A. Finke, H. Bußkamp, M. Manea, A. Marx, *Angew. Chem. Int. Ed.* **2016**, *55*, 10136 – 10140; *Angew. Chem.* **2016**, *128*, 10291 – 10295.

[17] a) S. Khetan, J. A. Burdick, *Soft Matter* **2011**, *7*, 830 – 838; b) X. T. Shi, S. Ostrovidov, Y. H. Zhao, X. B. Liang, M. Kasuya, K. Kurihara, K. Nakajima, H. Bae, H. K. Wu, A. Khademhosseini, *Adv. Funct. Mater.* **2015**, *25*, 2250 – 2259; c) C. Colosi, S. R. Shin, V. Manoharan, S. Massa, M. Costantini, A. Barbetta, M. R. Dokmeci, M. Dentini, A. Khademhosseini, *Adv. Mater.* **2016**, *28*, 677 – 684.

Manuscript received: October 16, 2016
Final Article published: ■■ ■■, ■■■■

Communications

DNA Hydrogels

J. Wang, J. Chao, H. Liu,* S. Su, L. Wang, W. Huang, I. Willner, C. Fan — ■■■–■■■

Clamped Hybridization Chain Reactions for the Self-Assembly of Patterned DNA Hydrogels

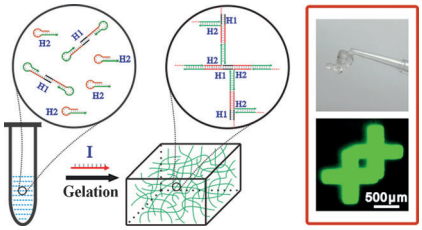

A clamped hybridization chain reaction (C-HCR)-based strategy is developed to guide DNA self-assembly to form macroscopic hydrogels. H1, H2 = DNA hairpin strands, I = initiator strand.

